The acceptance tests for the new Legnaro ECRIS 3

The PIAVE injector has been regularly working since 2004. The beams coming from PIAVE are now in the regular beam time schedule. The present ALICE ion source, core of PIAVE injector, is 15 years old and more than one generation of ECR ion sources have been developed in the meantime, offering far better performances in terms of intensity and charge states reached inside the plasma. The ECR ion sources are so widely use that, even if they still continue to be part of interesting research and technology programs, they have become a standard product on the accelerator technology market. In 2006 the Laboratori Nazionali di Legnaro decided to buy a new ion source to replace the old present ALICE: to keep as low as possible the power consumption of the system installed on the high-voltage platform, the choice fell on the permanent magnet Supernanogan source built by Pantechnik.

The new source, LEGIS, represents a step forward for the performances of PIAVE-ALPI complex. The experimental program of AGATA detector has been based mainly on the increased ion current and charge state available from LEGIS, therefore a first complete characterization of this new device was necessary.

3.1 ECRIS: brief introduction

Several general characteristics of ECR sources explain their widespread application in the accelerator community. Most important is the ability to produce CW beams from a lare variety of elements at useful intensities and good beam quality for nuclear and atomic physics research. The main characteristic of ECR sources is that the discharge in plasma is produced by RF power without cathodes. Therefore, only the source material injected into an ECR source is consumed. As a result, ECR sources can be operated continuously for long periods without interruption. Maintenance required on ECR sources is also minimal, consisting mainly of occasional repair of vacuum equipment, external ovens and electrical support equipment.

3.1.1 ECRIS characteristics

An ECR Ion Source (ECRIS from now on) consists of a vacuum chamber working as resonant cavity for microwaves (usually from 14-18 GHz), multiple solenoids for axial magnetic confinement, a multipole magnet (usually a sextupole) for radial confinement and an extraction system made usually of three electrodes for ion beam production. The microwaves are coupled to the source both on and off axis, via rectangular waveguides: they deliver the electromagnetic radiation which heats electrons through a process called Electron Cyclotron Resonance (ECR). The plasma electrons have two main components, a cold population (~20 eV) and a warm population with higher temperature; another population in the MeV range is also present (hot electrons) but it does not play any role in plasma ionization and dynamics due to the too high energy. Typical ion energies are a few eV. The electrons produce the high charge state ions primarily by sequential impact ionization. The ions and the electrons must be confined for sufficient time for the sequential

ionization to take place. In a typical ECRIS, the ion confinement times need to be about 10^{-2} s to produce high charge state ions. The ionization rate depends on the plasma density, which typically ranges from about 10^{11} cm^{-3} for low frequency sources to more that 10^{12} cm^{-3} for the highest frequency sources. Charge exchange with neutral atoms must be minimized, so operating pressures are typically 10^{-6} Torr or less. The plasma chamber is biased positively so that at extraction the ions can be accelerated out of the plasma and into the beam transport system.

The following sections [1] will briefly explain most of the topics related with ECRIS.

Electron Impact Ionization. In ECR sources multiply charged ions are created mainly by step-by-step ionization, caused by the successive impact of energetic electrons. Therefore the electron impact ionization cross sections are significant parameters.

Charge Exchange. The cross sections for charge exchange between highly charged ions and neutrals are extremely large. Typical charge exchange cross sections are three to four orders of magnitude larger than corresponding electron impact ionization cross sections. Fortunately, the reaction rates are proportional to the projectile velocities, and neutral atoms are much slower than warm electrons. Still, to keep the rate of production by electron impact equal to the rate of loss by charge exchange for high charge state ions, it is necessary for the neutral atom density in the plasma to be two orders of magnitude lower than the electron density.

Plasma confinement. The processes that govern particle confinement in an ECRIS are complex. The temperatures of electrons and ions are different and their confinement times vary considerably. Furthermore, the electron velocity distribution function consists of more than one population, usually described as cold, warm, and hot populations. Since the confinement times are proportional to the electron temperatures, they are different for each electron population. For what concerns ions, if their confinement time is too short, they do not have time to reach high charge states and if the confinement time is too long, the high charge state ions decay by charge exchange instead of being extracted as a useable beam.
Particles, which oscillate back and forth in the magnetic mirror, can be scattered into the so called loss cone in the velocity space by collisions. High energy electrons, which have low collision rates, are well confined. The cold electrons suffer more frequent scattering collisions and are less well confined. On the other hand, the ions are highly collisional and are therefore not magnetically confined. For high charge state ECR ion sources, simple axial mirrors do not provide sufficient magnetic confinement. In addition to the axial magnetic field produced by solenoids, the typical high charge state ECR source uses a sextupole (also called hexapole) or other multipole magnet to produce a radially-increasing field. The combination of the axial mirror field and the radial multipole field produces a "minimum-B" magnetic field configuration, where the magnetic field is minimum at the center of the device and increases in each direction away from the center to the chamber walls. Such a field provides a plasma confinement geometry that is stable against MHD instabilities. The ratio of the maximum field strength at the peak of the magnetic mirrors to the minimum field strength at the center of the device is defined as the axial mirror ratio, $R_m = B_{max}/B_{min}$. The ratio of the minimum field at the center of the plasma chamber to the maximum field at the plasma chamber wall (moving radially at midplane) defines the radial mirror ratio. While the early ECR ion sources operated with axial and radial mirror ratios with values less than two, the newer sources use mirror ratios as high as 4 at injection, 2 at extraction, and slightly greater than 2 in the radial direction. These higher mirror ratios improve the plasma confinement and this shifts the charge state distribution to a higher average charge.

ECR heating. To optimize the rate of ionization by electron impact, electron temperatures between 1 keV and 20 keV are typically needed. The ion temperature on the other hand should be as low as possible because the ion temperature is one source of ion losses and, once extracted, of emittance and energy spread in the extracted beam. Therefore, a method to selectively heat the electrons in the plasma is desirable. The use of ECRH meets this

requirement. If we introduce into the plasma an electromagnetic wave, whose frequency is equal to the cyclotron frequency of the electrons in the magnetic field, an extremely efficient energy transfer occurs between the wave and the electron population. In a minimum-B configuration, the magnetic field is not uniform but increases from the center to the outside. Therefore the ECR condition is normally met only on a closed surface around the center, called the "ECR surface", which must be closed inside the plasma chamber. For high performance ECR ion sources, the ECR surface sits well inside of the plasma chamber wall, which means high radial confinement performances.

Gas mixing. It was discovered during operation of ECR sources that the production of high charge state ions can be substantially enhanced by adding a light support or mixing gas (typically oxygen) to the ECR plasma. Normally about 80% mixing gas is used and it can be up to 95% or higher for very heavy elements. However, a too high ratio of mixing gas increases the neutral pressure inside the ECR plasma and may also limit the production of higher charge states and the maximum intensity of heavier ions. A widely accepted explanation of this effect is that energy is transferred due to collisions from the heavier ions to the light ones, increasing the confinement time for the former. In addition, the lighter ion also lowers the average charge of the plasma, which again increases the plasma confinement time.

3.1.2 Beam production

ECRIS can in principle ionize every atomic specie in gaseous form: typical gaseous beams are O^{6+}, Ar^{9+}, Kr^{15+}, Xe^{26+}. C^{4+} is now widely used in facilities for hadron therapy like CNAO in Pavia [2].

For those atomic species which are not gaseous at room temperature, different methods can be used to vaporize and then ionize such species:

Resistive oven Of all the methods for the production of metal ion beams, the oven technique is the least intrusive, especially if pure metals can be used. Generally, a metal vapor pressure of about 10^{-3} to 10^{-2} Torr is required inside the oven (for an oven aperture of about 3 mm diameter) to supply the right amount of atomic flux to the ECR plasma. The temperature needed to produce a particular metal ion beam can be estimated from the vapor pressure curve of the metal. Besides the temperature required to evaporate the metal, chemical compatibility of the hot liquid metal and the crucible must be considered. For metals with temperature requirements less than 1600 C ceramic inserts such as zirconia, alumina or yttria can be used to prevent alloying of the heating crucible with the molten metal. For higher temperatures, ceramics begin to sublime and can even react with the hot metals. Therefore, the material has to be either loaded directly into the W or Ta furnace or special crucibles must be used.

Sputtering system. For the sputtering technique, a sample is mounted axially or radially at the periphery of the plasma and is negatively biased with respect to the plasma. The sample is sputtered by the plasma ions, and neutral metal atoms diffuse into the ECR plasma where they are ionized. This technique partly decouples the ECR plasma from the evaporation process. However, adequate plasma density is required to ensure sufficient sputtering rate, and therefore the ion source tuning is not completely decoupled from the evaporation process. Furthermore, the achievable intensities are dependent on the sputtering yield. Thus the sputtering method is very convenient for low intensities, but has limitation for the production of high intensity metal beams.

Direct insertion. The direct insertion technique was one of the first to be utilized for a wide variety of metals and is still used by most ECR groups. A support gas such as oxygen sustains the plasma while a solid rod is positioned close to the plasma, where it is vaporized and the

vapor is subsequently ionized. Though the insertion technique is simple and effective, it has the operational disadvantage of strong coupling between plasma and sample heating. However, for some refractory metals (e.g., tantalum) it may be the only choice available. Stable operation can be achieved by carefully controlling the position of the rod.

MIVOC. In some cases, gaseous compounds can be used, especially if the components of the compound can serve as a good mixing gas. Generally, one has to look for compounds with light elements. Sulfur for example can easily be produced from SO2, CS2 or H2S. Oxygen is an excellent mixing gas, therefore a compound containing oxygen is best choice if the desired metal is heavier. If the desired metal is lighter than oxygen, hydrogen is the better choice. Carbon contaminates the plasma chamber walls and should be avoided whenever possible. The metallic compound is loaded into an external chamber and connected to the source by a leak valve. After the initial pump down of the residual gas in the MIVOC chamber, the compound vapor can be introduced into the source as an ordinary gas. The main advantage is the fast setup time and ease of use, but rare isotopes are often not readily available in the appropriate chemical form. Another major drawback is the impurities (in particular carbon) which contaminate the plasma chamber walls. The ion source performance and stability can be compromised, particularly for long duration, high intensity applications.

3.1.3 Beam extraction

In general an ion source consists of two parts. The first part is the plasma generator that provides ion production and thus serves as an ion reservoir. The second part is the extraction system for accepting ions from the reservoir and forming an ion beam. Both parts of the source may be treated independently as long as the plasma generator provides ions at the required current density and covers the whole area of the extraction system. The extraction system determines the beam properties such as ion current and beam quality in general.

Extraction system

Ion extraction from a charged particle reservoir, i.e. a plasma, and ion beam formation is done by a so-called extraction system. The extractor consists of a plasma electrode at positive potential and a ground electrode at ground potential. The electric field strength E is given by the voltage U and the distance d between plasma electrode and ground electrode. The emission surface of the ions at the plasma boundary is called the plasma meniscus. Electrons coming from the plasma are reflected at this boundary if their energy is less than the potential drop between the two electrodes.

The extracted ion beam current is either limited by emission or by space charge forces. For the second case the extractable emission current density can be calculated by the Child-Langmuir law. In this case the emission area is assumed to be planar and infinite, with ions having zero initial energy in the longitudinal direction (z-direction). Then

$$j_{CL} = \frac{4}{9}\,\epsilon_0 \sqrt{\frac{2e\zeta}{m}}\frac{1}{d^2}U^{3/2} \tag{3.1}$$

where ϵ_0 is the vacuum permittivity, e the electronic unit charge, ζ the ion charge state, m the ion mass, d the gap width, and U the potential drop. The electric field strength is given by $E = U/d$. The equation is strictly valid only for electrons coming from a fixed emitting area.

The total ion beam current that can be formed from a cylindrically-symmetric extraction system is then given by the expression

$$I_{CL} = \frac{4}{9}\pi\epsilon_0 \sqrt{\frac{2e\zeta}{m}}S^2U^{3/2} \tag{3.2}$$

where $S = r/d$ is the aspect ratio, r is the radius of the hole in the plasma electrode, and πr^2 is the emitting area.

For the case of a diode system, electrons that are generated within the beam channel are accelerated towards the plasma and may change the charge state distribution in the emission region. Furthermore, these electrons may not contribute to space charge compensation of the ion beam right behind the ground electrode. Without space charge compensation of the ion beam the divergence angles of the ion beam trajectories increase rapidly after extraction. Therefore a third electrode, the so-called puller, is placed between the plasma electrode and ground electrode, and held at a negative potential; this is called a three-electrode or triode extractor system. This electrode gives rise to a potential hump for these electrons. In the case of a triode system the absolute value of the negative potential has to be added to the potential used in the first equation.

Beam emittance

For an ECR extraction system two main contributions to the ion beam emittance have to be considered: the ion beam temperature and the induced beam rotation due to the decreasing axial magnetic field.

The emittance due to ion temperature can be estimated by assuming a Maxwellian temperature distribution inside the plasma [3]:

$$\varepsilon_{temp}^{rms,n} = 0.016\, r \sqrt{\frac{kT_i}{A/q}}, \tag{3.3}$$

where ε is the normalized $x - x'$ RMS emittance in mm mrad, r is the plasma outlet hole radius in mm, kT_i is the ion temperature in eV, and A/q is the ratio of ion mass in amu to ion charge state and is dimensionless.

Assuming an uniform plasma density distribution across the plasma outlet hole, the emittance due to beam rotation induced by the decreasing magnetic field in the vicinity of the extractor can be described by Busch's theorem [4], assuming 100% = 5 RMS (a waterbag distribution)

$$\varepsilon_{mag}^{rms,n} = 0.032\, r^2 B_0 \frac{1}{A/q}, \tag{3.4}$$

where ε is the normalized $x - x'$ rms emittance in mm mrad, r is the plasma outlet hole radius in mm, B_0 is the axial magnetic field strength at the extractor in T, and A/q is the ratio of ion mass in amu to ion charge state and is dimensionless.

Beam rotation due to the decreasing magnetic field becomes the dominating contribution to the ion beam emittance when the following condition, derived by combining the previous equations, is satisfied:

$$B_0\, r \geq 0.5 \sqrt{kT_i}\, \sqrt{A/q}, \tag{3.5}$$

where B_0 is in T, r is in mm, kT_i in eV, and A/q is dimensionless. The magnetic field is the main contribution to the ion beam emittance in most ECR ion sources.

In addition to the magnetic field at the extractor, the ion confinement in the plasma and plasma stability also play important roles in determining the ion beam emittance. Experimentally it has been found [5] that, within the charge state distribution for a particular element, the measured emittance decreases for higher charge states. The highly charged heavier ions appear to be concentrated more on the axis of the ion source showing an opposite behavior with respect to the Busch theorem, whereas the low charge state ions could also be produced in the outer shell of the ECR plasma.

Therefore, for the same plasma conditions and the same gap width, the increase of the extracted current in the Child-Langmuir regime depends quadratically on the radius of the hole as well as the emittance out of the hole. This means that the higher the extracted current, the higher the emittance. However the emittance out of the source, i.e. downstream the extraction, strongly depends also on the design of the extraction system itself. Taking into account that an ECRIS designed for nuclear physics experiments must be able to produce a large assortment of ion species with high charge state and quality, the extraction system is as important as the plasma confinement and ionization.

Table 3.1: Alice and LEGIS comparison table.

	Alice	LEGIS
microwave frequency	14.4 GHz	14.5 GHz
max. microwave power	350 W	700 W
axial field	up to 0.8 T	1.1 T
radial field at chamber wall	0.7 T	0.9 T
maximum extraction voltage	12 kV	30 kV
Ag	0.87 μA ($^{19+}$)	4 μA ($^{20+}$)
Ar^{9+}	10 μA	100 μA
Xe^{23+}	1 μA	14 μA

3.2 The PIAVE ion source upgrade

It comes out from the previous sections that the sensitive parameters of ECRIS sources in terms of ionization performances are the maximum confinement magnetic field B and the RF frequency f. In particular three empirical laws [6] describe how the performances in terms of charge state production and intensity are effected by the source design parameters:

$$q_{opt} \propto \log B^{3/2}, \qquad q_{opt} \propto \log f^{7/2} \qquad \text{and} \qquad I^{q+} \propto f^2,$$

where q_{opt} is the peak of the charge state distribution and I^{q+} is the current of the selected charge state. On the other hand the extracted current increases with RF power.

Keeping the RF frequency fixed, better performances are obtained increasing the confinement magnetic field and RF power. It is clear from the comparison table (Tab. 3.1) the reason why the Supernanogan has far better performances compared to the present Alice: to allow a higher maximum extracted current the extraction voltage is more than 100% higher as well as the microwave power and the confinement field. The results are that the noble gases are 10 times more intense and the example of a resistive oven ionized specie shows a factor of 4.

From the extraction system point of view, LEGIS foresees a four electrodes solution (see (1) in Fig. 3.2), the plasma electrode (24 kV), the puller (negative voltage), a lens electrode (positive voltage) and the ground electrode. To reach high performances, the puller and the lens voltage must be tuned for every ion specie.

In Tab. 3.2 the LEGIS guaranteed beam currents are reported. Note that the metallic ions like Ta are produced via sputtering whereas Ag, Au, Pb with the resistive oven.

Figure 3.1 shows the charge q and the A/q ratio of a sample of ions extracted from Supernanogan. The features of these ions are I $\geq$ 1 μA and 4 $\leq$ A/q $\leq$ 7, this to ensure that they can be transported and stripped as described in Chapter 4 with a final current greater than 1 pnA. Therefore it is possible to characterize the LEGIS-Supernanogan ion production from this point of view with a simple formula,

$$q = (-0.0025\, Z + 0.57)\, Z, \tag{3.6}$$

which will be useful in Section 5.6, even though lacking of a real physical meaning.

3.3 LEGIS acceptance tests

To be sure that the higher current is not obtained to the detriment of beam emittance (as reported in Tab. 2.1 the acceptance of the PIAVE SRFQs is less than 0.9 mm mrad norm.) a proof of the beam quality was required.

Table 3.2: Supernanogan guaranteed intensities (μA). The cells in gray represents the sample of ions plotted in the graph below.

	1+	2+	4+	6+	8+	9+	11+	14+	18+	20+	21+	23+	26+	27+	30+
H	2000														
^{2}H	2000														
^{3}H	700														
He	2000	1000													
C	500	350	200	3											
N	1000	300	100	10											
O	1000	400	300	200											
Ne	1000	300	200	160	25										
Ar	1000	350	250	200	200	90	30	1							
Cu						3	5	2							
Kr	1000						25	15	1						
Ag			250	250	200	90	30		4		3				
Xe	500				220					15		14	5	3	
Ta										4	0.8				
Au													10	6	1
Bi												5	7	5	1

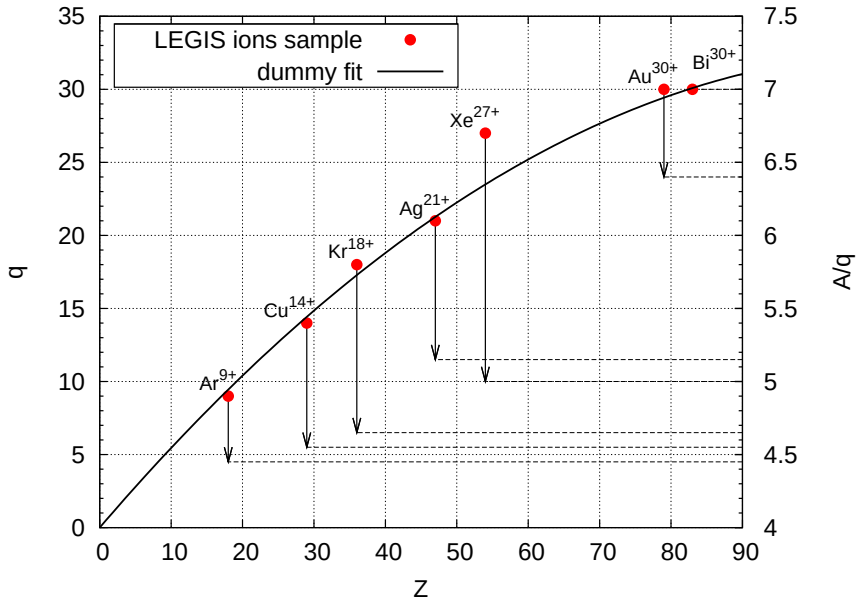

Figure 3.1: Sample of Supernanogan ions charge state as function of the atomic number Z. The sample characteristics are I ≥ 1 μA and 4 ≤ A/q ≤ 7. The dummy fit will be used in Section 5.6 to describe the performances of the various upgrade scenarios in case of the stripping foil option. Each arrow points to the A/q value for the ion whom it refers to.

Table 3.3: Supernanogan LNL requested performances by contract.

beam	ion	I (μA)
gaseous	Ar^{9+}	100
	O^{6+}	200
metallic from sputtering	Ta^{24+}	1
metallic from oven	Ag^{21+}	3
	Au^{26+}	10
	Au^{30+}	1

3.3.1 LNL requests by contract

By contract a beam current stability two-hours test was required. During the test the current read by the Faraday cup had to stay within ±5% of the currents reported in Tab. 3.3 except for maximum 2% of the time (less than 4 mins). The operator could tune the source to recovery the current after a blackout or to increase its stability during the test for a maximum of 15 mins. An additional specification on beam quality was required for O^{6+}, Ar^{9+} and Au^{26+} ion beams: the measured normalized 4 RMS emittance for 90% of the beam current had to be lower than 0.3 mm mrad. To determine the 90% value a threshold is applied to the acquired data so to have the 90% of the requested current.

The gaseous beams chosen for the test are the easiest beams which the source can provide and therefore they will be the first extracted beams once the source will be installed on the platform at LNL. Ta^{24+} is the only metallic beam generated via sputtering on the Supernanogan guaranteed beams list. The tests on the metallic beams from oven are very important to check the performances of the oven itself. The reason of three kind of beams is evident: Ag^{21+} is a medium mass easy to vaporize beam, Au is a heavy beam with an ionized q/A which gives 7.6 for 26+ and 6.6 for 30+, where only the latter could work for the ALPI upgrade described in Chapter 5.

3.3.2 The LNL test bench at Pantechnik

The LEGIS test bench at Pantechnik comprises:

1. the ion source and the 4 electrodes extraction system (plasma electrode, puller, lens to analysis and ground electrode);
2. the slits placed after the extraction system which cut the external part of the beam. In such a way the total transported current diminishes but the beam selected by the dipole has better emittance for a given current (preliminary tests by Pantechnik);
3. the analysis dipole, 90 degree bend and 400 mm radius;
4. the emittance-meter consisting of a variable slit and a independently moving wire. The control system provides the step value, the slit dimensions (which are set equal to intercept the entire beam without overlapping) and the wire sampling points number. The slits are used to increase the A/q resolution as well.
5. the Faraday cup, 30 mm diameter.

The extraction voltage was set to 24 kV for all the extracted beam. In Tab. 3.4 all the main characteristics for beam optics are reported. This test bench represents at its best the situation on PIAVE platform so to make easier the first tests on-site. The set-up of the emittance-meters has a spatial resolution of 0.5 mm and can resolve 1.25 mrad. This choice was made to have a comparable

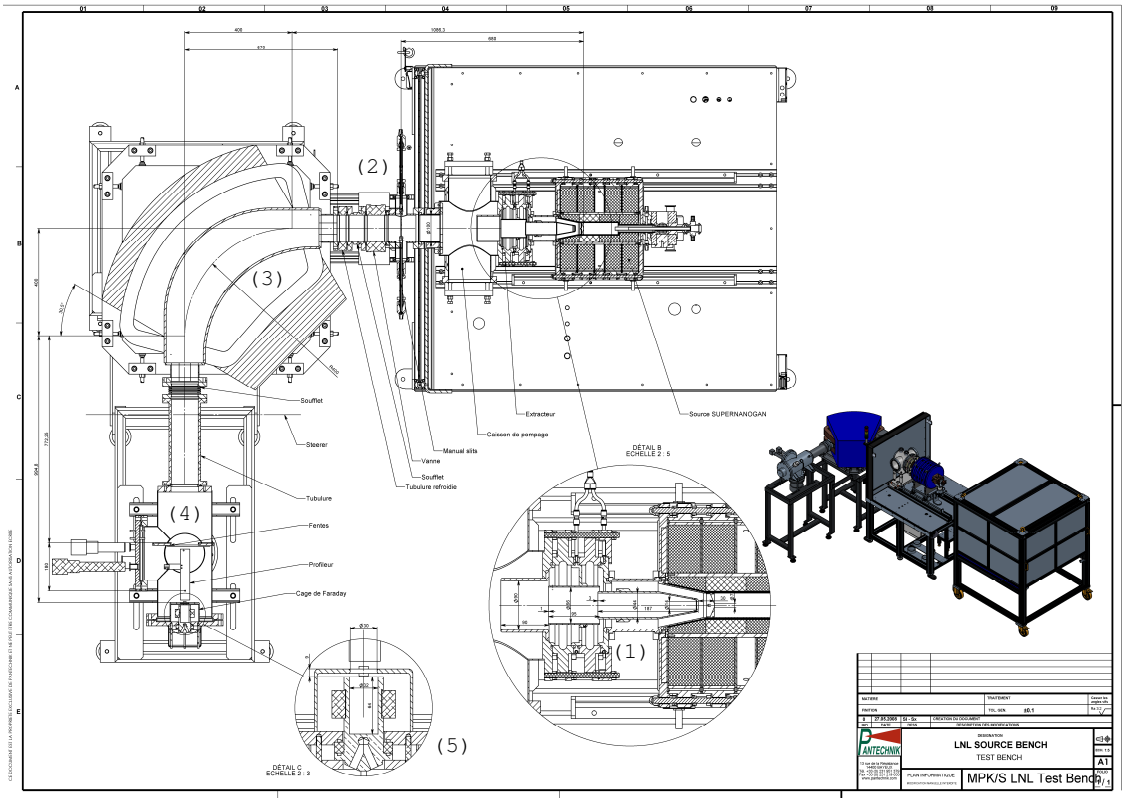

Figure 3.2: The LNL test bench at Pantechnik company. (1) extraction system, (2) slits, (3) analysis dipole, (4) emittance-meter and (5) Faraday cup.

Table 3.4: Pantechnik test bench details.

extraction gap (mm)	30
dipole edges (deg)	30.5
plasma electrod to dipole (mm)	1120.6
plasma electrod to slit (mm)	704.8
dipole to slit (mm)	780
slit to wire (mm)	180
dipole to Farady Cup (mm)	1002.6
slit step = slit width (mm)	0.5
wire step (mm)	0.25

Table 3.5: LEGIS source settings during the test.

	Ar^{9+}	O^{6+}	Ta^{24+}	Ag^{21+}	Au^{26+}	Au^{30+}
puller voltage (V)	0	-210	-371	-25	-385	-582
lens voltage (V)	922	882	875	1020	948	1040
power (W)	166	177	177	190	444	384
total extracted current (mA)	3.1	4.6	1.8	3.1	2.5	2.3
Bias voltage (V)	-382	-368	-546	-212	-558	-469
Bias current (mA)	1.47	2.20	2.39	1.29	1.32	1.15
slit diameter (mm)	28	30	open	open	open	open

number of non-zero data in space and angle taking into account the beam characteristics at the emittance-meter slits and the 10 % discard of the data due to emittance calculation threshold.

The emittance data were officially analyzed by a Pantechnik developed program but the raw data were also independently analyzed at LNL. Therefore it has been possible to check other parameters, like the halo [7] and the emittance population.

3.3.3 The tests

During the tests, as shown in Fig. 3.5, the source was tuned each time to reach the requested current. The mixing gas for all the beams was Oxygen except for O^{6+} test, that was performed with Helium. To improve the beam transport from the extraction system to the dipole the use of the slits was envisaged even though not supported by simulations. After the emittance measurements it was also checked whether the full current was read by the Faraday cup. For this reason the acquired distributions were transported through a program developed at LNL (see Fig. 3.4) to the Faraday cup and no losses in the x plane were found.

Ar^{9+} The first beam tested on Supernanogan was Ar^{9+}. The requested current was 100 μA with an 4 RMS normalized emittance less than 0.3 mm mrad for 90% of the beam.
After a long conditioning of the source the beam was ready to begin the two-hours test (see Fig. 3.3(a)). The reference current was 101 μA and it was out of the ±5% limit for 38 s (0.52%). The results of the emittance measurements were also within the limits.
From Tab. 3.6 and from the comparison between Fig. 3.5(a) and Fig. 3.5(a) it can be seen that the beam had different characteristics before and after the two-hours test: the beam centroid changed by 2 mm (this could be explained taking into account the spectrum acquisition in between) and the emittance by 20% probably because of changed plasma conditions.

O^{6+} The LNL request was 200 μA with a 4 RMS normalized emittance less than 0.3 mm mrad for 90% of the beam. In Fig. 3.3(b) the two-hours stability test is shown: the reference current was 205 μA and the ±5% limit was exceeded for 75 s (1.04%).
Table 3.6 shows the results of the two emittance measurements of O^{6+}: the value of 195 μA is due to a reduction of the extracted current during the measurement; anyway the 90% emittance corresponding of the required current (180 μA) satisfies the specifications. The analysis of Tab. 3.6 and Fig. 3.6 shows that the beam conditions were steady and the peak has become more intense loosing part of the halo.

Ta^{24+} The test with the sputtering probe was made just after the O^{6+} test. The requested current was 1 μA and no emittance measurement was required. The performed current was 1.45 μA and the ±5% limit was exceeded for 26 s (see Fig. 3.3(c)).

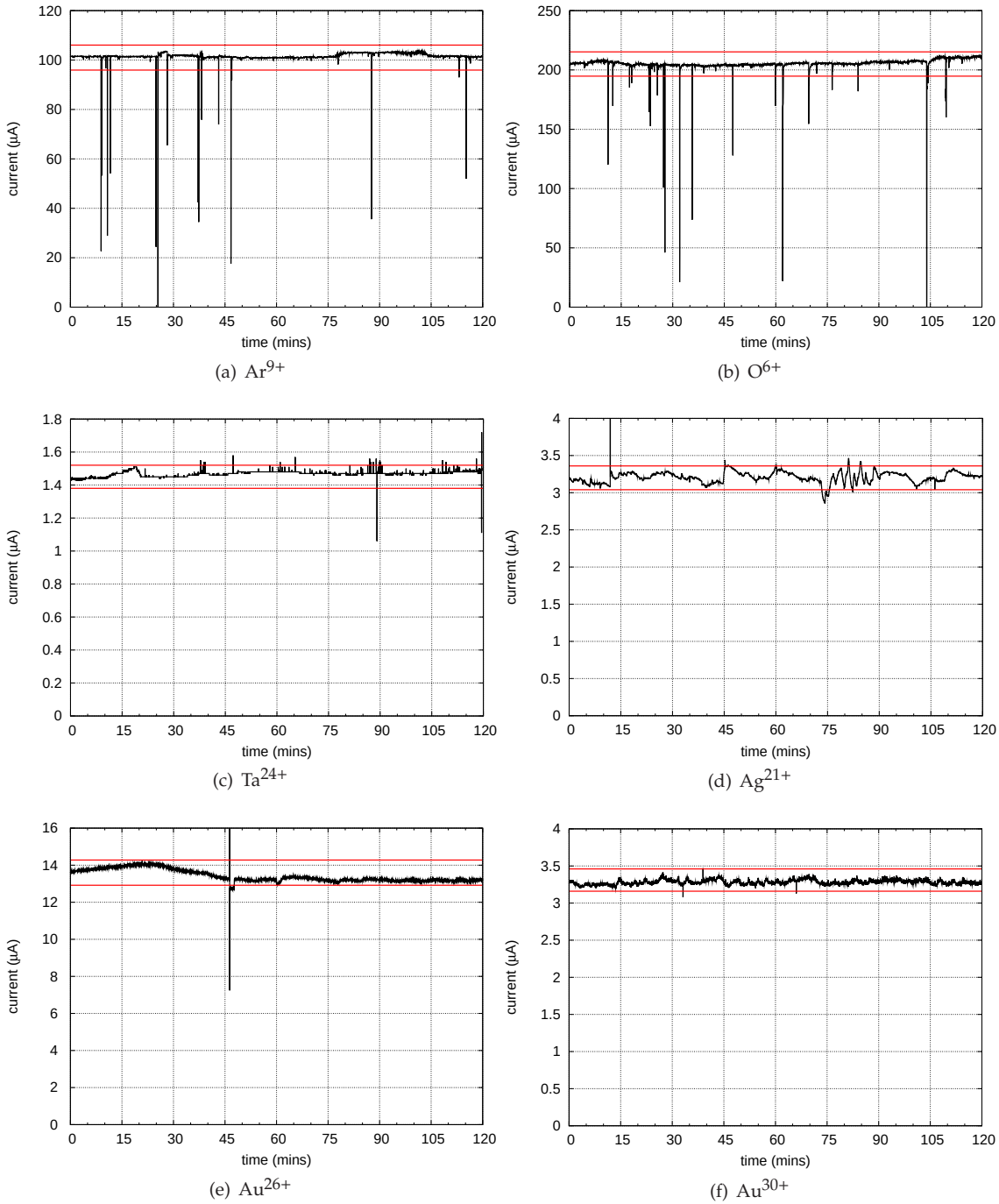

(a) Ar^{9+} (b) O^{6+}

(c) Ta^{24+} (d) Ag^{21+}

(e) Au^{26+} (f) Au^{30+}

Figure 3.3: Two-hours current stability tests summary. All the tests were fully successful.

Table 3.6: Emittance measurements results. The units are mm mrad.

ion		I (μA)	4 $\epsilon_{rms\ 100\%}$	4 $\epsilon_{rms\ 90\%}$	4 $\epsilon_{rms\ 90\%\ n}$	α_x	β_x	$< x >$	$< x' >$	$H_{100\%}$	$H_{90\%}$
Ar^{9+}	*start*	105	87	48	0.163	-0.32	0.48	-0.32	4.88	1.79	0.97
	end	102	97	59	0.200	0.07	0.43	1.72	7.73	1.83	1.20
O^{6+}	*start*	195	87	65	0.285	-0.39	0.49	0.94	5.11	1.46	0.62
	end	211	87	52	0.228	-0.23	0.35	0.86	6.04	1.50	0.38
Au^{26+}	*end*	13.6	47	39	0.103	2.29	0.56	0.45	7.46	0.60	0.76

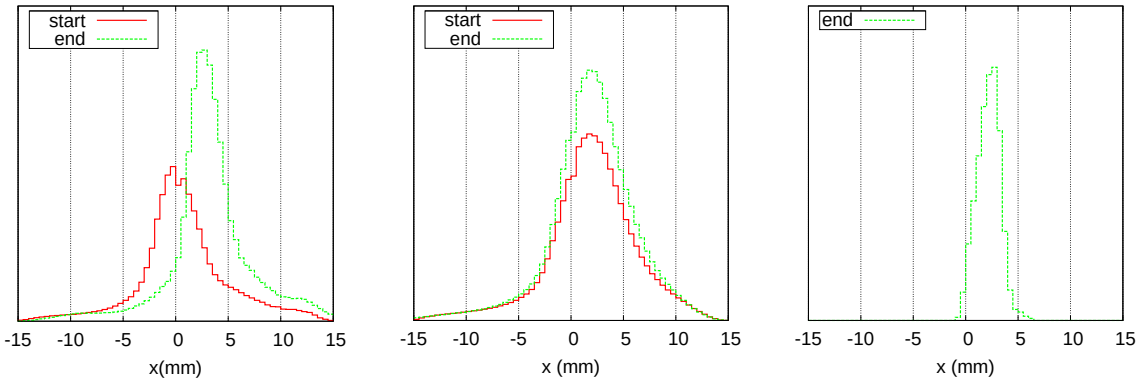

(a) Ar^{9+} (b) O^{6+} (c) Au^{26+}

Figure 3.4: Beam profiles at Faraday cup. The horizontal axis extremes represent the Faraday cup width.

Ag^{21+} During the beam preparation some problems arose from the oven crucible: the evaporation had to be repeated three times before reaching sufficient current and stability. The crucible was filled with natural abundance Ag: for this reason both the isotopes ^{107}Ag and ^{109}Ag were present. Unfortunately the bending dipole was not able to resolve clearly the isotopes. To check that the sum of the current of both isotopes was at least the requested value, the use of the slits of the EMD was necessary. The selected window was ±2 mm for the check and opened up to ±8 mm for the test. The reference current for the final stability test in Fig. 3.3(d) was 3.4 μA and the limit was exceeded for 2.9% of the time: the test was failed and it was necessary from Pantechnik to fix the weak points of the system.

Au^{26+} and Au^{30+} After the problems came out with Ag, the oven head was redesigned and built. The stability of the oven improved significantly and even if the Au required an higher temperature, the tests were performed without any difficulty. The stability test (see Fig. 3.3(e) and 3.3(f))was successful: 99% of the time for Au^{26+} and almost 100% for Au^{30+} within the ±5% limit. The emittance measurement was foreseen just for 26+ ion and was performed only after the stability test. The 4 RMS normalized emittance was one third of the requested value.

3.3.4 Conclusions

The tests were successful for all the requested beams, however it is worth to underline some points. During the test with gaseous beams the great importance of source conditioning clearly came out: even if the produced ions had low masses, it was difficult to reach an adequate current stability because of plasma instabilities due to a great outgassing of plasma chamber. In fact the

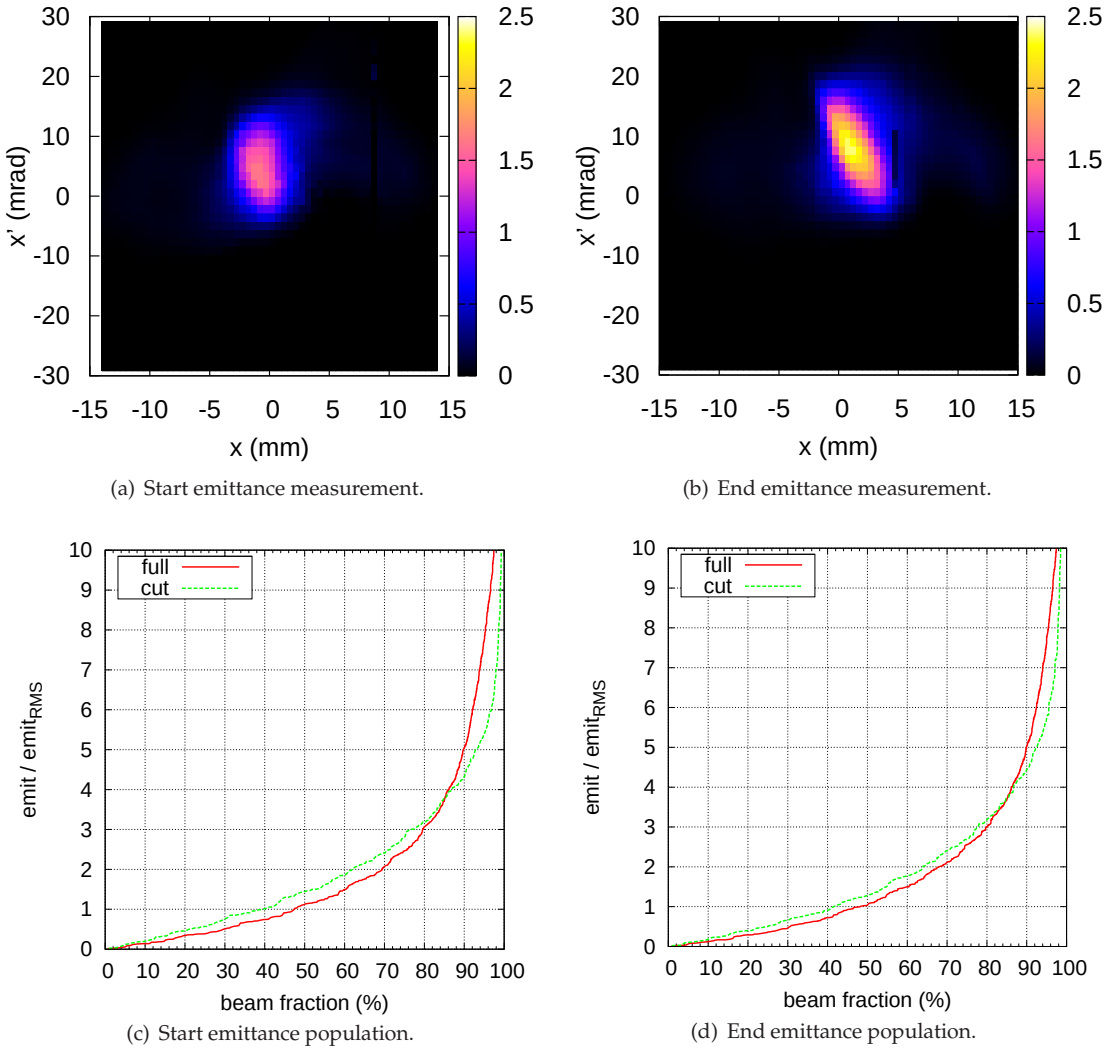

(a) Start emittance measurement.

(b) End emittance measurement.

(c) Start emittance population.

(d) End emittance population.

Figure 3.5: Ar^{9+} graphical summary.

fraction of neutral particles inside the plasma strongly influences source performances following the multiply charged ion production criterion [8]. The plasma chamber conditioning normally requires hundreds hours of continuous operation, whereas the tests independently performed by Pantechnik on LEGIS were limited. Concerning the sputtering system, the LNL requests were not so stringent in terms of current and charge state taking into account the usual low yield of such an evaporation technique. It must be mentioned as well that the A/q value for Ta^{24+} is 7.54, too high to be accelerated in the PIAVE-ALPI complex.

Beam emittance

As reported in [9], for a given kind of ions the emittance decreases increasing the charge state. It was also found that, fixing an A/q value, the emittance decreases increasing the mass. The first phenomenon reveals an opposite A/q dependence with respect to theory as if highly charged heavier ions were concentrated more on the axis of the ion source and so extracted from a smaller hole. The discrepancy between experimental and theoretical data increases decreasing A/q. The second phenomenon shows a mass dependence of the emittance hiding the influence of space

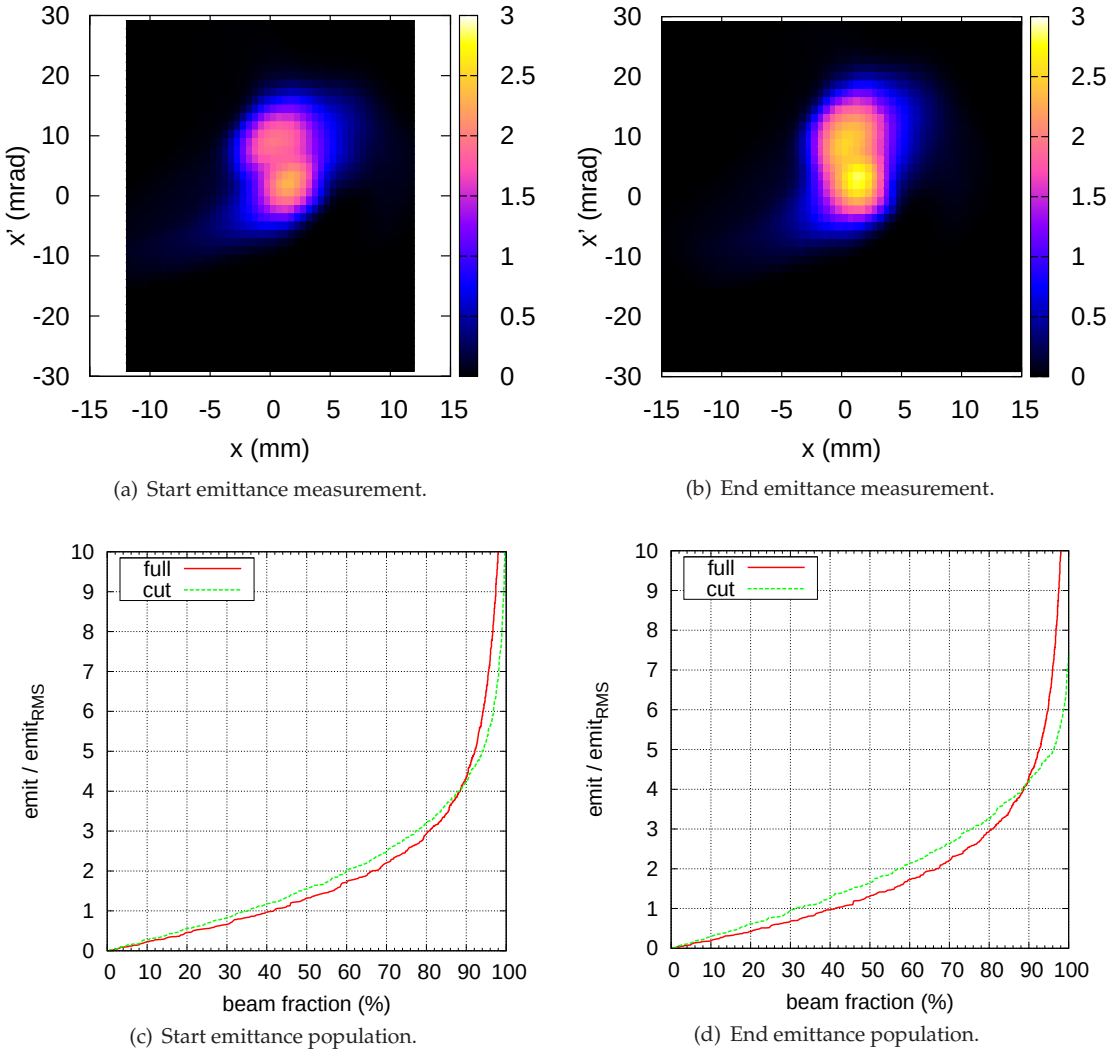

(a) Start emittance measurement.

(b) End emittance measurement.

(c) Start emittance population.

(d) End emittance population.

Figure 3.6: O^{6+} graphical summary.

charge. It is widely known in fact that, fixing the A/q value, increasing mass means increasing charge states and, consequently, charge exchange probability. For this reason the neutral particles component must be kept lower resulting in a lower extracted and transported current.

The measured emittances (see Tab. 3.7) are lower than the values obtained with Eq. 3.4. In particular the discrepancy is higher for O^{6+} having the lower A/q value. The minimum emittance is measured for Au^{26+}, which is the heaviest one and was obtained producing the lowest extracted current. Direct comparison between measurements is not so meaningful because they are obtained by different plasmas.

Bibliography

[1] R. Geller and al., "Electon Cyclotron Resonance Ion Sources: historical review and fututre prospects," *Review of Scientific Instruments*, vol. 69, no. 3, 1998.

[2] http://www.cnao.it/.

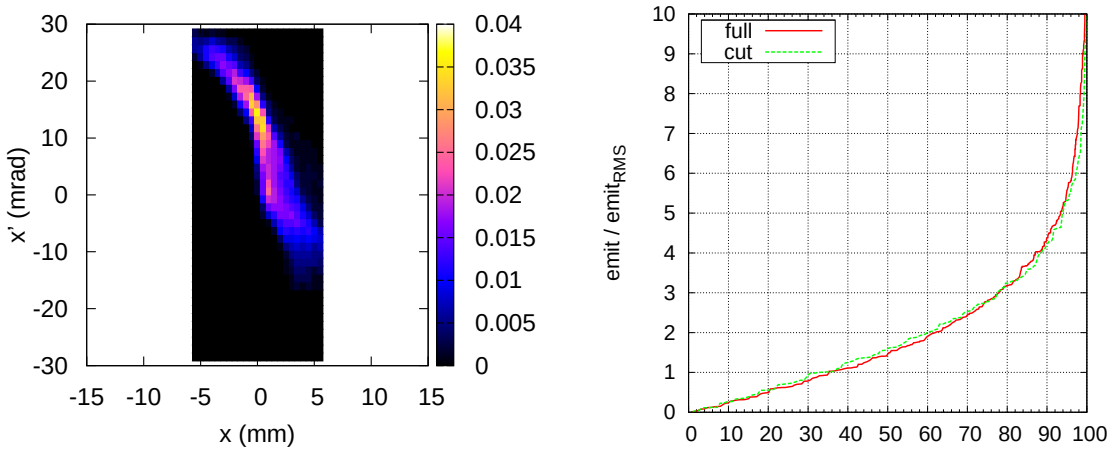

(a) End emittance measurement.

(b) End emittance population.

Figure 3.7: Au^{26+} graphical summary.

Table 3.7: Comparison between expected (from Eq. 3.4) and measured emittance best values (in mm.mrad.norm).

ion	A/q	I_{tot} (mA)	ϵ_{rms} th.	ϵ_{rms} exp.	*var.*
O^{6+}	2.67	4.6	0.118	0.057	*-51%*
Ar^{9+}	4.44	3.1	0.071	0.041	*-42%*
Au^{26+}	7.58	2.5	0.041	0.026	*-38%*

[3] P. Allison, J. D. Sherman, and H. . Smith Tech. Rep. LA-8808-MS, Los Alamos National Lab, 1981.

[4] A. Septier, *Focusing of Charged Particles*. New York: Academic Press, 1967.

[5] D. Wutte, M. Leitner, and C. M. Lyneis *Physica Scripta*, no. T92, p. 247, 2001.

[6] T. A. Antaya and S. Gammino, "The superconducting electron cyclotron resonance 6.4 ghz high-b bode and frequency scaling in electron cyclotron resonance ion source," *Review of Scientific Instruments*, vol. 65, no. 1723, 1994.

[7] C. K. Allen and T. P. Wangler, "Beam halo definitions based upon moments of the particle distribution," *Phys. Rev. ST Accel. Beams*, vol. 5, p. 124202, Dec 2002.

[8] R. Geller, *Electron Cyclotron Resonance Ion Sources and ECR plasmas*. Philadelphia: Institute of Physics Publishing, 1996.

[9] C. Lyneis and D. Leitner, "ECR Ion Sources," in *The Physics and Technology of Ion Sources* (I. Brown, ed.).